This is a repository copy of *Image-based ex vivo drug screen to assess targeted therapies in recurrent thymoma*.

White Rose Research Online URL for this paper:
http://eprints.whiterose.ac.uk/160541/

Version: Published Version

Image-based *ex vivo* drug screen to assess targeted therapies in recurrent thymoma

Antti Arjonen[a,1], Rami Mäkelä[a,1], Ville Härmä[a,b], Nina Rintanen[c], Teijo Kuopio[c],
Juha Kononen[c,d], Juha K. Rantala[a,b,*]

[a] *Misvik Biology Oy, Turku, Finland*
[b] *University of Sheffield, Sheffield, UK*
[c] *Jyväskylä Medical Centre, Jyväskylä, Finland*
[d] *Docrates Cancer Center, Helsinki, Finland*

ARTICLE INFO

ABSTRACT

Objectives: Thymoma is a rare malignancy derived from the thymic epithelial cells. No standard salvage treatments are available for recurrent thymoma and due to the low number of cases, alternative treatment regimens have been assessed only in small case series with varying success. The aim of this study was to use an image-based *ex vivo* drug screening strategy to assess efficacy of a large panel of anti-cancer agents for thymoma using patient derived tumor cells.

Materials and Methods: Vital tumor and tumor associated cells were used to assess the efficacy of 147 anti-cancer drugs including approved and experimental agents. Drug efficacy was analyzed at single cell resolution using image-based high content drug screening to assess tumor cell specific responses. Molecular profiling and histopathology was used to confirm the drug targets identified by the screen.

Results: The *ex vivo* drug screen identified selective sensitivity of the cancerous epithelial thymoma cells to EGFR-, HDAC- and mTOR-inhibition. Histopathology confirmed high protein level expression of EGFR in the patient's tumor. Patient was initiated treatment with Cetuximab resulting in stable disease after relapse on five different chemotherapy regimens.

Conclusion: The results show that the image-based *ex vivo* therapy efficacy screening strategy can be used to identify patient and tumor relevant drug sensitivity patterns in thymoma. The results also warrant continued research on EGFR as a biomarker and therapy target in recurrent thymomas.

1. Introduction

Thymus is a small gland located beneath breastbone. It is part of the lymph system and plays a key role in adaptive immune system with a function to produce and mature lymphocytes. Thymoma is a subtype of thymic epithelial tumors (TET) originating from the thymic epithelium from thymus gland. Based on the incidence rate of 0.15 cases per 100 000, thymoma is classified as a rare cancer [1]. Thymomas are best known for their association with myasthenia gravis, a neuromuscular junction disease related to skeletal muscle weakness [2]. Staging of thymomas is widely based on the Masaoka-Koga system [3] and the American Joint Committee on Cancer (AJCC TNM) staging system that

is based on the combined efforts by the International Thymic Malignancy Interest Group (ITMIG) and the International Association for the Study of Lung Cancer (IASLC) [4]. In short, these staging systems are based on the local micro- and macroscopic invasion of the tumor to surrounding fatty tissue and neighboring organs, together with the indicators of the presence of lymphogenous and hematogenous metastases with definition of various subtypes associated with different morphological features and clinical outcomes. On basis of the first clinical practice guideline for thymomas, released late 2019 (National Comprehensive Cancer Network, version 1.2020), surgical resection (thymectomy) combined with radiotherapy has a key role in the treatment of thymomas though diversity of opinion on treatment

approach exist [5]. The outcome, recurrence rate and survival of patients after thymectomy varies depending on the stage of the cancer, with the stage, the extent and completeness of resection and the histological classification being most significant prognostic factors [6]. For example, 10–20 year survival rates for Masaoka stages I and II is > 80 % with recurrence rate of 0.9–4.1 % respectively. Stage III shows 30–85 % and stage IV < 58 %, with 28.4, and 34.3 % reported recurrence rate [7,8]. For recurrent, unresectable thymomas, no standard salvage treatments are currently available after failure of standard chemotherapy and the low number of cases limits systematic assessment on novel therapies. Thus, new modern therapeutic approaches that have shown efficacy in initial clinical studies including targeting HDAC- [9], mTOR- [10], EGFR- [11], VEGFR- [12] and PD-1 [13] should be studied further in order to increase later-stage thymoma outcomes

In this study, we report an image-based *ex vivo* screen to assess drug efficacy on metastatic thymoma cells and to inform treatment of the patient after the standard treatments had been exhausted. High-throughput drug screening with vital patient derived cell cultures makes it possible to assess therapeutic efficacy of hundreds of drugs in parallel [14,15]. It is thus an attractive application for biomarker discovery and assessment of patient and tumor type specific therapy sensitivity especially in context of rare cancers such as metastatic thymoma, for which alternative approaches to better stratify patients to matched targeted therapies are currently unavailable [16].

2. Materials and methods

2.1. Patient

The patient, a 54-year old female, was identified to the study by an oncologist at the Jyväskylä Medical Centre (Jyväskylä, Finland). She was initially diagnosed with thymoma at age 43 with associated myasthenia gravis and treated by thymectomy followed with azathioprine for symptom control. One year after the thymectomy a recurrent disease was diagnosed and the patient received cisplatin-epirubicin as first line systemic chemotherapy. Regimen had to be stopped due to side effects and patient was given radiation therapy to mediastinum (ad 50 Gy) followed by four rounds of carboplatin as single agent. 3 years after initial diagnosis a new surgery of tumor mass at retroperitoneum was performed followed by treatment with four rounds of carboplatin-etoposide regimen. Following relapse, the regimen was changed to pemetrexed achieving a stable disease for 3 years. 9 years after initial diagnosis, metastatic disease was detected in the ovaries and the patient was treated with surgery followed by pemetrexed and ifosfamide treatments as single agents. 11 years following initial diagnosis the patient was diagnosed with multiple separate mediastinal tumor masses (maximum dimension of largest mass 7 cm), a paravertebral tumor next to left kidney and tumor mass affecting left pleura. She was then considered for detailed molecular pathology profiling and the *ex vivo* therapy sensitivity study. A tissue biopsy was collected for the *ex vivo* drug screening in context of palliative surgery with approval from the local Ethics Committee of the Central Finland Health Care District (KSSHP 3U/2015). All the experiments were undertaken with the understanding and written consent of the patient and the study methodologies conformed to the standards set by the Declaration of Helsinki.

2.2. Tumor derived primary cell culture

The surgical tissue sample from the metastatic lesion was divided into two halves of which other was used for histopathology processing and the other for the *ex vivo* screening (Fig. 1). Collected directly from the surgery, the live tissue sample was rinsed with sterile PBS and finely cut to $1-2 \, mm^3$ pieces in sterile RMPI-1640 (Gibco) cell culture medium using scalpels. The primary bulk cell suspension dissociated from the tumor tissue during cutting was collected into a sterile

centrifuge tube. The remaining tissue fractions where then placed into 1 mL of Accutase cell dissociation reagent (Gibco) and incubated at room temperature for 60 min. Following the enzymatic disaggregation, the resulting cell suspension and the initial cell suspension from the tissue cutting plates were combined into a milieu of normal, cancerous, immune and other native microenvironmental cell types, collected with centrifugation and subjected to filtration through a 70 μm cell strainer (pluriSelect Life Science UG) in sterile RMPI-1640 medium. The resulting cell suspension was quantified using a Cellometer Mini cell counter (Nexcelom) and diluted to RPMI-1640 medium containing 5 % FBS to achieve a suspension with 2500 cells per 45 μL of medium. Cells were then seeded directly onto the drug containing 384-well plates to initiate the 72 h drug exposure in standard cell culture conditions (37 °C, 5 % CO_2).

2.3. Mutation analysis

The genomic profiling was performed at the Jyväskylä Medical Centre molecular pathology core (Jyväskylä, Finland). Briefly, genomic DNA was extracted from representative FFPE tissue sections with QIAamp DNA FFPE Tissue Kit (Qiagen) according to the protocol provided by the kit manufacturer. Qiaseq Human Comprehensive Cancer Panel (Qiagen, DHS-3501Z) including 275 cancer related genes was used to prepare NGS amplicon gene library according to the protocol provided by kit manufacturer. Unique molecular identifiers (UMI) were used to tag individual DNA strands. Sequencing was performed with Illumina NextSeq500 instrument (Illumina, San Diego, CA, USA) according to standard protocol. Data was de-multiplexed and fastq files created with bcl2fastq software (Illumina). The data was processed in CLC Biomedical Genomics Workbech (Qiagen) with workflow provided by Qiagen and using Hg19 human reference genome to call the gene variants. Gene annotations were performed according to the vcf files in OmnomicsNGS software (Euformatics, Espoo, Finland).

2.4. High content imaging drug screening

The therapeutic compound collection used in the drug screening consisted of 147 anti-cancer agents, purchased from a commercial chemical vendor (Selleck biochemicals). The *ex vivo* drug screening was performed on tissue culture treated 384-well microplates (Corning). Each compound was tested in four different concentrations with 2-fold dilutions starting from 5 micromolar as the highest concentration. A single-cell suspension of freshly isolated tumor derived cells (45 μL per well; 2500 cells per well) was transferred to each well using a peristaltic dispenser (ThermoScientific). The 384-well plates were incubated for 72 h in standard cell culture conditions. Analysis of cell viability with cellular lineage separation was performed through high-content imaging. The cell cultures were fixed with 4% paraformaldehyde supplemented with 0.3 % Triton-X100 and incubated overnight at +4 °C with antibodies against epithelial cell marker cytokeratin-19 (KRT19, Abcam, Clone EP1580Y) and stromal mesenchymal cell marker vimentin (VIM, Santa Cruz Biotechnology, Clone V9). Secondary antibody staining was performed at room temperature for 1 h with AlexaFluor-labelled secondary antibodies against the primary host species (1:500, LifeTech) in 1% BSA. 1 μg/mL DAPI (4′,6- Diamidino-2-phenylindole nuclear counterstain, LifeTech) was added to secondary staining buffers for DNA counterstaining. Cells were imaged using Olympus scanˆR platform at 20× magnification. 9 images were acquired from each 384-well to cover the whole well area. Images were analyzed with Olympus scanˆR image analysis suite including integrated DNA staining-based primary object segmentation using a watershed algorithm. Primary objects (nuclei) were expanded a fixed 20-pixel distance, and mean fluorescence signal intensity for KRT19 and VIM was quantified from this expanded cellular region. Single cell positivity for KRT19 and VIM were determined by gating in the scanˆR image analysis suite, using cells negative for each marker as controls.
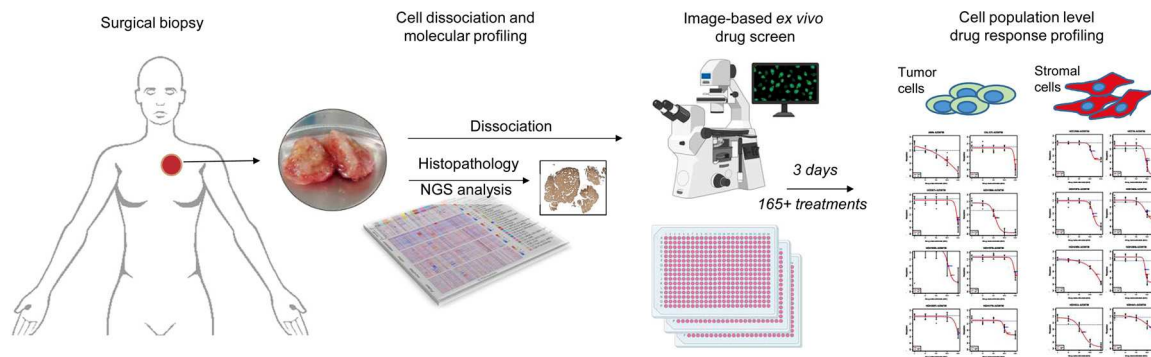
Fig. 1. Overview of the *ex vivo* high content image-based drug screening strategy. Patient derived tissue sample was used for molecular pathology and the drug screening. Drug screening of 147 drugs was performed with high content microscopy to allow cell type specific drug response profiling.

Population separated cell count data was normalized to DMSO-only wells (negative control), 5μM staurosporin-containing wells (positive control) and 2μM aphidicolin-containing wells (cell growth control). Dose response curves and for growth rate normalized GR50 and IC50 estimates were generated in GraphPad Prism software (V8, GraphPad Software Inc.).

2.5. Statistical analysis

The *ex vivo* drug screening data was analyzed using the normalized growth rate inhibition (GR) approach which yields per-division metrics for drug potency and efficacy. The normalized growth rate inhibition (GR) method corrects for variation in division rates by estimating the magnitude of drug response on a per cell-division basis [17,18]. The GR values were used for comparison of drug potency between the KRT19$^+$ and VIM$^+$ cell populations having a differential proliferation rate during the screening. GR values were calculated using:

– *x(c)*, the cell count value of a cell population per well following drug treatment at concentration *c*.

– x_{ctrl}, the average cell count value of a cell population in DMSO-treated control wells from the same plate; x_{ctrl} = mean({xi∈x | abs (log10(xi)–log10(mean(x)))o1.5)}) where x are all DMSO treated control values.

– x_0, the average cell count value of a cell population in 2μM Aphidicolin treated control wells from the same plate; x_0 = mean({xi∈x | abs(log10(xi)–log10(mean(x))) o1}) where x is the vector of treated values.

Supplementary data 1 comprises the GR values for each treated condition of all cells and the KRT19$^+$ and VIM$^+$ cell populations calculated as follows:

$$GR(c) = \frac{\log_2 \left(X(c)/X_0 \right)}{2^{\log_2 \left(\frac{X_{ctrl}}{X_0} \right)} - 1}$$

Cell state frequencies were calculated using the Olympus scanˆR imaging cytometry software (Olympus OSIS, Germany) as described above. Welch's *t*-test and Pearson correlation analyses were applied using GraphPad Prism V8 software according to assumptions on data normality.

3. Results

3.1. Ex vivo drug efficacy screening in patient derived thymoma cells

The tumor sample for the *ex vivo* drug screening was obtained from a bronchial metastatic lesion of a 54-year old female patient with a metastatic thymoma with pleural invasion. Histopathologic evaluation of the tumor tissue (Supplementary Fig. 1) confirmed type B3 thymoma with supporting immunohistochemical profile of negative staining of CD5 and CD117 and positive staining of p63 (TP63) [19], strong

positive epithelial cell staining of KRT19 (cytokeratin-19) [20] and spatially restricted staining of VIM (vimentin) [21] and KRT14 (cytokeratin-14) [20] surrounding the blood vessels (Supplementary Fig. 1). For the *ex vivo* screening, the tissue sample was processed into a single cell milieu of tumor derived cells immediately on the day of surgery as described in detail in section 2.2. The disaggregated cells were exposed to 147 drugs in four different doses for 72 h and high content image-based analysis approach was used to assess the cytotoxic effects of the drugs (Fig. 1). Based on the immunohistochemical evaluation of the tumor tissue, the epithelial cell marker KRT19 [20] was selected as a marker for the thymic epithelial cells and VIM for tumor derived stromal cells [21] to allow cell type stratified analysis of the drug responses (Supplementary Fig. 2). Aphidicolin was used as a growth stalling non-cytotoxic reference molecule (Supplementary Fig. 2B) to monitor and normalize the dose responses of the KRT19$^+$, VIM$^+$ and all cells with respect to growth rate (GR) during the assay [17,18]. In the DMSO treated control samples, 55.2 % of all analyzed cells were KRT19$^+$ and 26.7 % VIM$^+$ (Supplementary Fig. 2B). The estimated cell doubling rate of all the tumor tissue derived cells was calculated to be ~200 h, KRT19$^+$ cells had a doubling rate of ~250 h and VIM$^+$ cells ~400 h corresponding to 0.34, 0.28 and 0.18 cell divisions over the course of the 72 -h screening assay respectively [22] (Supplementary Fig. 2B). To identify the most potent cell type selective growth inhibitory drugs, we compared the GR dose response metrics of the drugs between the KRT19$^+$ cells, VIM$^+$ cells and all cells (Fig. 2A). Using a stringent ranking criterion where the average of the GR values across all four drug doses (GR$_{mean}$) had to be less than GR < -0.1 (mean - standard deviation of aphidicolin samples), we identified 17 drugs associated with a cytotoxic effect on all cells, 19 drugs with higher efficacy on the KRT19$^+$ cells and 20 drugs with higher efficacy on the VIM$^+$ cells (Fig. 2A).

3.2. Analysis of cell type selective drug efficacy

The image-based assay strategy allows analysis of dose responses at single-cell resolution for stratification effects on cell population level. The efficacy of the drugs between the KRT19$^+$ and the VIM$^+$ cells varied most for the response to epidermal growth factor receptor (EGFR) tyrosine kinase inhibitors (Fig. 2A-C) indicating selective efficacy dependent on the cell type (IC$_{50}$, p = 0.0001, Fig. 2D). 5 out of the 7 EGFR inhibitors included in the analysis had a cytotoxic effect (GR < -0.1) on the KRT19$^+$ cells, 1 had a low growth inhibitory effect and 1 (Gefitinib) had a weak growth inhibitory effect (Fig. 2B & E). On the VIM$^+$ cells, none of the EGFR inhibitors resulted in a significant cytotoxic efficacy (Fig. 2B-E). Pan-EGFR inhibitor AZD8931 [23] showed highest efficacy of all the EGFR inhibitors on the KRT19$^+$ cells with an estimated IC$_{50}$ of ~630 nM (Table 1). Other agents displaying high efficacy on the KRT19$^+$ cells and lower efficacy on the VIM$^+$ included HDAC inhibitors Belinostat and Panobinostat, Bcl-2 inhibitor
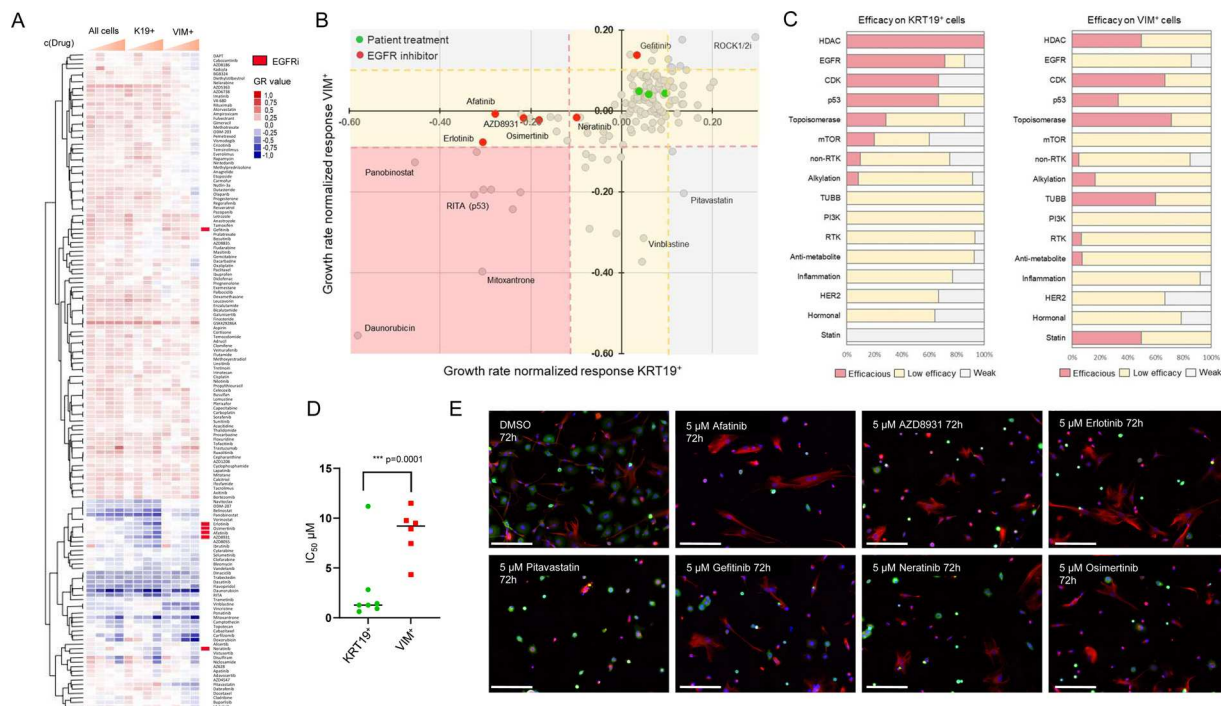
Fig. 2. Results of the *ex vivo* drug screening in thymoma cells. **A.** One dimensional (vertical) unsupervised clustering of the growth rate normalized dose responses of all cells, KRT19$^+$ and VIM$^+$ cells. Four of the included EGFR-TKI drugs (red indicator) cluster together with lower GR values in the tumor cells (GR < 0 in blue). **B.** Correlation of the GR$_{mean}$ values of all drugs between KRT19$^+$ and VIM$^+$ cells. EGFR-TKI drugs shown in red, patient's treatments prior to test shown in green. **C.** Distribution of drug efficacy at drug class level on KRT19$^+$ and VIM$^+$ cells based on the response classes defined by efficacy. GR$_{mean}$ < -0.1 = Efficacious, GR$_{mean}$ < 0.1 = Low efficacy and GR$_{mean}$ > 0.1 = Weak efficacy. **D.** Comparison of the micromolar IC$_{50}$ estimates of the seven included EGFR-TKI on KRT19$^+$ and VIM$^+$ cells (p = 0.0001). **E.** Imaging of the cell type specific responses to EGFR-TKI and Pitavastin in comparison DMSO treated cells. KRT19 staining shown in green and VIM staining in red. DNA counterstaining shown in blue. Scale bars 100 μm (For interpretation of the references to colour in this figure legend, the reader is referred to the web version of this article).

Table 1
Growth rate normalized analysis-yielded estimates for IC50 (μM) of the epidermal growth factor receptor (EGFR) tyrosine kinase inhibitors.

Drug name	All cells	KRT19+	VIM+
Afatinib	4.79	1.28	8.92
AZD8931	7.95	0.63	4.33
AZD9291	6.62	1.45	9.51
Erlotinib	7.63	0.91	11.51
Gefitinib	33.23	11.19	n/a
Ibrutinib	4.85	1.28	7.46
Neratinib	9.03	2.82	9.77

Navitoclax, bromodomain inhibitor ODM-207 and mTOR inhibitors Vistusertib and AZD8055 (both dual specific inhibitors of MTORC1 and MTORC2). Topoisomerase inhibitors, tubulin poisons, Pitavastatin, a statin and Sunitinib, an angiogenesis inhibitor had higher efficacy on the VIM$^+$ cells (Fig. 2B,C,E). None of the drugs the patient had received as treatment; carboplatin, cisplatin, etoposide or pemetrexed had a cytotoxic response on either the KRT19$^+$ or the VIM$^+$ cells (Fig. 2B). The cytotoxic effect of RITA, an inhibitor of MDM2-p53 interaction, on both the KRT19$^+$ and VIM$^+$ cells suggested a p53 wild-type genetic background [24]. The GR normalized drug screening data is provided as supplementary data 1 (DOI: 10.17632/cy579t8dcr.1).

3.3. Ex vivo informed treatment

Based on the *ex vivo* drug screening results, the KRT19$^+$ epithelial tumor cells were selectively sensitive to EGFR inhibitors as an individual class of drugs (Fig. 2C-D). High expression levels and genomic aberrations of EGFR was recently reported in a subset of type B3 thymoma patients [25]. In earlier studies, two individual thymoma cases

were reported where Cetuximab anti-EGFR therapy resulted in stable disease [26,27], and Erlotinib showed clinical efficacy in the initial trial [28], but the only case report on using Gefitinib for treatment of recurrent thymoma described no clinical benefit [29]. To assess whether the patient's tumor cells' sensitivity to the EGFR inhibitors was due to possible mutations in the EGFR pathway, molecular pathology analysis including NGS and immunohistochemistry was performed from the tumor tissue. Targeted sequencing of pathogenic variants of 275 cancer related genes identified no EGFR aberrations and only one other aberration with known clinical significance; an AR (androgen receptor) c.2395C > G (p.Gln799Glu) mutation with 52 % mutant allele frequency. Immunohistochemistry analysis revealed strong uniform membranous staining of EGFR across the tumor tissue (Fig. 3A-B). Based on this finding, and the earlier reports describing successful use of EGFR-TKI therapy to treat patients with recurrent thymoma [26–28], the patient was considered for treatment with EGFR-TKI. After clinical evaluation, the patient was started on Cetuximab therapy [26,27]. Clinical benefit from this therapy was apparent already at the first planned control one month after initiation of therapy (Fig. 4). The progression of the disease during treatment with Ifosfamide included accumulation of pleural fluid, mediastinal tumor masses and atelectasis (Fig.4A). Radiographic examination after 4 month of treatment with Cetuximab indicated that pleural fluid and atelectasis had not returned and the mediastinal mass delineated better and was marginally smaller thus confirming a radiologically stable disease (Fig. 4B). During further follow-up the patient continued to derive clinical benefit from Cetuximab for 13 months at which point CT scans showed unequivocal progression of the disease with new metastatic lesions (Fig. 4C). At that point, patient was switched to best palliative care and received radiation therapy to painful disease lesions. She succumbed to disease shortly after stopping of active treatment.
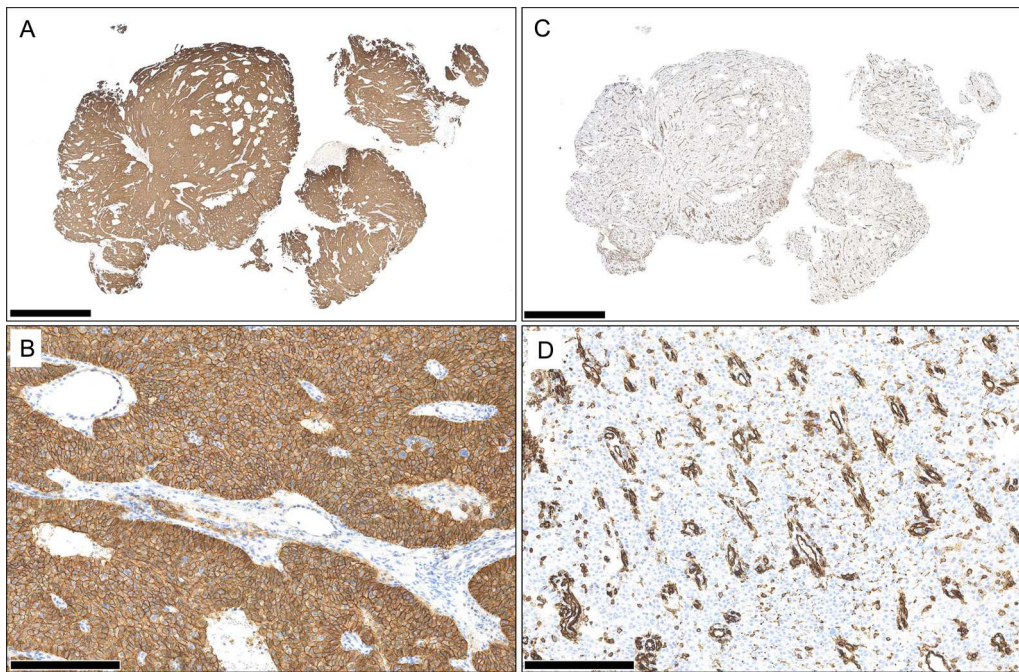
Fig. 3. Immunohistochemistry of the tumor tissue. **A.** EGFR staining of the whole section. **B.** 20× magnification of the EGFR staining. **C.** CD31 staining of the whole section. **D.** 20× magnification of the CD31 staining. Scale bars. A,C: 2.5 mm, B,D: 250 µm.

4. Discussion

Thymoma is a rare type of cancer, but comprises the most common primary tumor of the anterior mediastinum. Recurrent malignant thymomas are also rare, but the incidence increases with stage of the disease from < 1% up to ~50 % [8]. High stage thymoma with mobile disease is associated with a poor prognosis and no salvage treatment following relapse on standard chemotherapies is available. To improve outcomes and efficacy of treatment of recurrent and/or refractory thymoma, research on alternative treatments have been started [10,13,30]. However, significant variation has been described in the response rates between individual patients and good biomarkers to guide therapy are lacking. Epidermal Growth Factor Receptor (EGFR) targeted therapies have been suggested as potentially efficacious treatments in advanced thymoma supported by reports of clinical benefit on individual patient cases with Cetuximab and the initial clinical trial of Erlotinib [26–28]. Partial responses in subsets of thymoma patients have also been achieved with treatments using histone deacetylase inhibitor Belinostat [9], mTOR inhibitor Everolimus [10] and angiogenesis inhibitor Sunitinib [12]. All of these drug classes displayed cell type selective efficacy in the *ex vivo* screening. EGFR, HDAC and mTOR inhibitors showed highest efficacy on the KRT19^{+} epithelial tumor cells. VEGFR inhibitor Sunitinib had a selective growth inhibitory effect on the vimentin expressing cells. VEGFR-TKI

treatments are thought to result in tumor regression primarily through the anti-angiogenic effects mediated by targeting the tumor vasculature composing cell types [12]. In the patient's tumor, both vimentin staining and staining of the vascular endothelial cell marker CD31 (Fig. 3C-D) localized to the cells lining the vasculature suggesting the VIM^{+} cells to be represent vascular endothelial cells. This shows that the image-based *ex vivo* therapy efficacy screening approach can be used to assess cell type specific drug responses with high precision. By identifying the response of the patient derived tumor cells to EGFR-TKI therapeutics, the technique helped to guide the pathological and clinical diagnostics resulting in confirmation of high EGFR expression in the patient's cancer. Standard therapeutic options had been exhausted for the patient and the analysis thus yielded a treatment option that would otherwise not have been considered for the patient. The significance of our study is thus its demonstration that rapid *ex vivo* screening without prior *in vitro* propagation of the patient derived tumor cells can be used to find clinically relevant information on drug sensitivity. This is particularly promising in context of rare cancers, for which large clinical studies are not possible due to low number of cases. In the future, combination of diagnostic therapy efficacy screening with sequencing and genomic information [14] could provide a robust diagnostic approach for personalized cancer medicine.
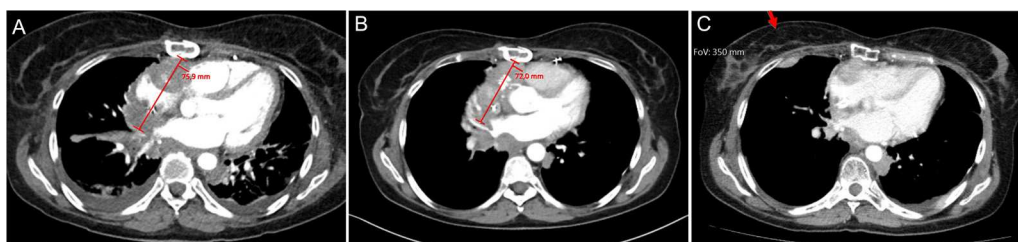

Fig. 4. Radiologic response of patient. **A.** Prior to treatment. Pleural fluid and atelectasis in addition to mediastinal tumor mass (measured 75.9 mm). **B.** After 4 month of treatment with Cetuximab. Pleural fluid and atelectasis have disappeared. Mediastinal mass delineates better and is sharper, marginally smaller (measured 72 mm). **C.** After 13 months of treatment with Cetuximab. Pleural fluid has reappeared along new lesions, such as one pointed out with the arrow in the image.

5. Conclusions

In summary, by interrogating drug sensitivity of patient-derived tumor cells *ex vivo*, we identified EGFR inhibitors as potential therapeutic option for the patient with a metastatic thymoma. Since several EGFR-TKI therapeutics are available in the clinic, and responses of thymoma patients EGFR-TKI therapies have been reported previously [26–28], histopathology analysis of EGFR should be considered as a predictive biomarker when selecting among treatment options to patients affected with recurrent or refractory thymoma. The results also suggest that thymoma cells can be sensitive to HDAC, bromodomain, Bcl-2 and mTOR inhibition warranting further study of these targeted therapeutics in context of recurrent thymoma.

Availability of data and materials

All data from the *ex vivo* drug screening is available through the Mendeley data repository (DOI: 10.17632/cy579t8dcr.1). Access to the tissue samples is available provided ethical approval and sample availability.

CRediT authorship contribution statement

Antti Arjonen: Methodology, Data curation, Formal analysis, Writing - original draft, Writing - review & editing. **Rami Mäkelä:** Conceptualization, Methodology, Data curation, Formal analysis, Validation, Writing - original draft, Writing - review & editing. **Ville Härmä:** Data curation, Writing - review & editing. **Nina Rintanen:** Resources, Data curation, Writing - review & editing. **Teijo Kuopio:** Resources, Data curation, Formal analysis, Validation, Writing - review & editing. **Juha Kononen:** Resources, Conceptualization, Data curation, Formal analysis, Validation, Supervision, Writing - original draft, Writing - review & editing. **Juha K. Rantala:** Resources, Conceptualization, Methodology, Data curation, Formal analysis, Validation, Supervision, Writing - original draft, Writing - review & editing.

Declaration of Competing Interest

The authors of this manuscript have no conflicts of interest to disclose. Juha K. Rantala is the founder of Misvik Biology Oy.

Appendix A. Supplementary data

Supplementary material related to this article can be found, in the online version, at doi:https://doi.org/10.1016/j.lungcan.2020.04.036.

References

[1] P.A. Zucali, L. Di Tommaso, I. Petrini, et al., Reproducibility of the WHO classification of thymomas: practical implications, Lung Can. 79 (2013) 236–241.

[2] F. Romi, Thymoma in myasthenia gravis: from diagnosis to treatment, Autoimmune Dis. 2011 (2011) 474512.

[3] F.C. Detterbeck, K. Stratton, D. Giroux, et al., The IASLC/ITMIG Thymic Epithelial Tumors Staging Project: proposal for an evidence-based stage classification system for the forthcoming (8th) edition of the TNM classification of malignant tumors, J. Thorac. Oncol. 9 (Suppl 2) (2014) S65–72.

[4] C.A. Moran, S. Suster, The World Health Organization (WHO) histologic classification of thymomas: a reanalysis, Curr. Treat. Options Oncol. 9 (2008) 288–299.

[5] E. Ruffini, F. Guerrera, A. Brunelli, et al., Report from the European society of thoracic surgeons prospective thymic database 2017: a powerful resource for a collaborative global effort to manage thymic tumours, Eur. J. Cardiothorac. Surg. 55 (4) (2019) 601–609.

[6] F. Venuta, M. Anile, D. Diso, et al., Thymoma and thymic carcinoma, Eur J. CardioThorac Surg Off J Eur Assoc Cardio-Thorac Surg 37 (2010) 13–25.

[7] J.F. Regnard, P. Magdeleinat, C. Dromer, et al., Prognostic factors and long-term results after thymoma resection: a series of 307 patients, J. Thorac. Cardiovasc. Surg. 112 (2) (1996) 376–384.

[8] K. Kondo, Y. Monden, Therapy for thymic epithelial tumors: a clinical study of 1,320 patients from Japan, Ann. Thorac. Surg. 76 (3) (2003) 878–884.

[9] G. Giaccone, A. Rajan, A. Berman, et al., Phase II study of belinostat in patients with recurrent or refractory advanced thymic epithelial tumors, J. Clin. Oncol. 29 (2011) 2052–2059.

[10] P.A. Zucali, T. De Pas, G. Palmieri, et al., Phase II study of Everolimus in patients with thymoma and thymic carcinoma previously treated with cisplatin-based chemotherapy, J. Clin. Oncol. 36 (4) (2018) 342–349.

[11] G. Farina, M.C. Garassino, M. Gambacorta, et al., Response of thymoma to cetuximab, Lancet Oncol. 8 (5) (2007) 449–450.

[12] A. Thomas, A. Rajan, A. Berman, et al., Sunitinib in patients with chemotherapy-refractory thymoma and thymic carcinoma: an open-label phase 2 trial, Lancet Oncol. 16 (2015) 177–186.

[13] J. Cho, H.S. Kim, B.M. Ku, et al., Pembrolizumab for patients with refractory or relapsed thymic epithelial tumor: an open-label phase II trial, J. Clin. Oncol. 37 (24) (2019) 2162–2170.

[14] K.I. Lehtomaki, L.I. Lahtinen, N. Rintanen, et al., Clonal evolution of MEK/MAPK pathway activating mutations in a metastatic colorectal Cancer case, Anticancer Res. 39 (11) (2019) 5867–5877.

[15] K. Kettunen, P.J. Boström, T. Lamminen, et al., Personalized drug sensitivity screening for bladder Cancer Using conditionally reprogrammed patient-derived cells, Eur J Urol 76 (4) (2019) 430–434.

[16] L. Billingham, K. Malottki, N. Steven, Research methods to change clinical practice for patients with rare cancers, Lancet Oncol. 17 (2) (2016) e70–e80.

[17] M. Hafner, M. Niepel, M. Chung, P.K. Sorger, Growth rate inhibition metrics correct for confounders in measuring sensitivity to cancer drugs, Nat. Methods 13 (2016) 521–527.

[18] M. Hafner, M. Niepel, P.K. Sorger, Alternative drug sensitivity metrics improve preclinical cancer pharmacogenomics, Nat. Biotechnol. 35 (2017) 500–502.

[19] M.A. den Bakker, A.C. Roden, A. Marx, M. Marino, Histologic classification of thymoma: a practical guide for routine cases, J. Thorac. Oncol. 9 (Suppl 2) (2014) 125–130.

[20] M. Kojika, G. Ishii, J. Yoshida, et al., Immunohistochemical differential diagnosis between thymic carcinoma and type B3 thymoma: diagnostic utility of hypoxic marker, GLUT-1, in thymic epithelial neoplasms, Mod. Pathol. 10 (2009) 1341–1350.

[21] B.A. Alexiev, C.B. Drachenberg, A.P. Burke, Thymomas: a cytological and immunohistochemical study, with emphasis on lymphoid and neuroendocrine markers, Diagn. Pathol. 2 (2007) 13.

[22] M. Hafner, L.M. Heiser, E.H. Williams, M. Niepel, N.J. Wang, J.E. Korkola, et al., Quantification of sensitivity and resistance of breast cancer cell lines to anti-cancer drugs using GR metrics, Sci. Data 4 (2017) 170166.

[23] D.M. Hickinson, T. Klinowska, G. Speake, et al., AZD8931, an equipotent, reversible inhibitor of signaling by epidermal growth factor receptor, ERBB2 (HER2), and ERBB3: a unique agent for simultaneous ERBB receptor blockade in cancer, Clin. Cancer Res. 16 (4) (2010) 1159–1169.

[24] N. Issaeva, P. Bozko, M. Enge, et al., Small molecule RITA binds to p53, blocks p53-HDM-2 interaction and activates p53 function in tumors, Nat. Med. 10 (12) (2004) 1321–1328.

[25] T. Sakane, T. Murase, K. Okuda, et al., A mutation analysis of the EGFR pathway genes, RAS, EGFR, PIK3CA, AKT1 and BRAF, and TP53 gene in thymic carcinoma and thymoma type A/B3, Histopathology 75 (5) (2019) 755–766.

[26] G. Palmieri, M. Marino, M. Salvatore, et al., Cetuximab is an active treatment of metastatic and chemorefractory thymoma, Front Biosci 12 (2007) 757–761.

[27] G. Farina, M.C. Garassino, M. Gambacorta, N. La Verde, G. Gherardi, A. Scanni, Response of thymoma to cetuximab, Lancet Oncol. 8 (2007) 449–450.

[28] P.M. Bedano, S. Perkins, M. Burns, et al., A phase II trial of erlotinib plus bevacizumab in patients with recurrent thymoma or thymic carcinoma, J. Clin. Oncol. 26 (2008) 19087.

[29] T. Nakagiri, S. Funaki, Y. Kadota, et al., Does gefitinib have effects on EGFR mutation-positive thymoma? Case report of thymoma recurrence, Ann. Thorac. Cardiovasc. Surg. 20 (2014) 674–676.

[30] B. Hu, B. Rong, Y. Han, Q. Li, Do thymic malignancies respond to target therapies? Interact. Cardiovasc. Thorac. Surg. 20 (2015) 855–859.